

# 1 Benefits of Electrified Propulsion for Large Aircraft

---

Rodger Dyson, Ralph Jansen, and Nateri Madavan

## Introduction

Three main questions are addressed in this book:

- (1) What are the benefits of electrified propulsion for large aircraft?
- (2) What technology advancements are required to realize these benefits?
- (3) How can the aerospace industry transition from today's state of the art to these advanced technologies?

This chapter addresses the first question, making the case for electrified aircraft propulsion (EAP) through numerous trade studies and the analysis of several concept vehicles. This will lay the groundwork for the chapters that follow, which – while remaining focused on question 1 – collectively address questions 2 and 3 in technical detail.

There is substantial interest in the investigation of improvements to aircraft efficiency through the introduction of electrical components into the propulsion system. In the case of turboelectric and hybrid electric aircraft, the electrical systems provide unmatched flexibility in coupling the power generation turbines to the fan propulsors. This flexibility facilitates tight propulsion–airframe integration and can result in reduced noise, emissions, and fuel burn. However, the greatly expanded electrical system incurs substantial weight and efficiency penalties at odds with its benefits. A promising intermediate step between a conventional turbofan aircraft and a fully turboelectric or electric aircraft is an aircraft with a partially turboelectric or hybrid electric propulsion system. Initial studies show that significant aerodynamic benefits can be achieved by sourcing just a small fraction of the propulsive power electrically. However, it is difficult to arrive at authoritative conclusions since the concept aircraft configurations thus far considered and many of the major electrical system components have yet to be built or verified.

In this chapter a breakeven analysis is presented to elucidate the electrical power system performance requirements necessary to achieve electrified aircraft propulsion – specifically fully turboelectric, partially turboelectric, and parallel hybrid electric. This first-order analysis provides a framework for comparing electric drive system performance factors, such as the electrical efficiency, in the context of aircraft propulsion systems. The value of this analysis is both to guide electrical system component research and to provide aircraft configuration researchers with reasonable component expectations.

Similar parametric analyses were presented previously for a fully turboelectric propulsion system [1] and a partially turboelectric system [2]. The study summarized here investigates a broader array of aircraft types, including the fully and partially turboelectric aircraft already addressed, as well as parallel hybrid electric aircraft. In the cases of partially turboelectric and hybrid electric systems, the fraction of thrust power will be varied between the turbofan engines and electric distribution to additional propulsors. A key difference between this study and the prior studies is in the breakeven analysis assumptions. Here the input power and ratio of operating empty weight to aircraft initial weight are held constant among the aircraft types, in addition to equating the range and payload weight. The other studies held either the initial aircraft weight or the fuel weight, as well as the operating empty weight, to be the same.

## 1.1 Benefits and Costs of Electrified Aircraft Propulsion

### 1.1.1 Benefits of Electrified Aircraft Propulsion

The turboelectric aircraft propulsion-derived system benefits have been described in previous papers by Jansen et al. [1, 2], and the main points are now summarized. Higher propulsive efficiency due to increased bypass ratio (BPR), higher propulsive efficiency due to boundary layer ingestion (BLI), and lift-to-drag ratio ( $L/D$ ) improvements are facilitated by EAP.

The introduction of an electric drive system between the turbine and fan enables the decoupling of their speeds and inlet/outlet areas. With this approach, high BPR can be achieved since any number and size of fans can be driven from a single turbine. Increasing BPR results in improved propulsive efficiency. Also, the speed ratio between the turbine and the fan can be arbitrarily set and varied during operation, thereby removing the physical constraint levied by either direct shaft or geared coupling. As a result, the fan pressure ratio and the turbine/compressor ratios can be optimized independently. The propulsive efficiency benefits due to higher BPR could be as high as 4–8 percent [3, 4].

BLI increases propulsive efficiency by ingesting lower velocity flow near the airframe into the propulsors, reenergizing the wake, and thereby reducing drag. BLI can be implemented on both conventional tube-and-wing and hybrid wing body (HWB) aircraft. The propulsor is mounted such that the slow-moving flow near the aircraft is ingested, reenergized, and exhausted where the aircraft wake would have been. The BLI benefits to propulsive efficiency are expected to be 3–8 percent [4, 5]. Combining BPR and BLI propulsive efficiencies listed here yields improvements of 7–17 percent.

Distributed propulsion is expected to improve both lift and  $L/D$  ratio through wing flow circulation control. The propulsors can be distributed above or below, or embedded in the traditional tube-and-wing configuration. Likewise, HWB configurations can employ fans distributed across or embedded within the upper surface. Improvements

in  $L/D$  ratio may result in smaller wing area and reduced drag and weight. The benefits of lift augmentation can be taken in reduced wing area for a given load capacity or shorter takeoff distances. Reduction in wing area lowers wing weight and drag, thereby imparting fuel savings. Alternatively, the improved lift could be focused on increased climb rate and reduced takeoff distance in order to decrease the noise footprint around the airfield. The  $L/D$  ratio could be improved by 8 percent [6] to 16 percent [5].

### 1.1.2 Costs of Electrified Aircraft Propulsion

Introducing an electric drive system, with or without batteries, into the aircraft propulsion system will add weight and reduce efficiency. Here, the electric drive system includes the electric machines, the power management and distribution system, and the thermal system related to heat removal in the two prior systems. Specifically, the electric drive system could include generators, rectifiers, distribution wiring, fault protection, inverters, motors, and the thermal control for those components.

The United States National Aeronautics and Space Administration (NASA) is investigating high-performance motors and batteries that could make electrified aircraft propulsion viable. With regard to the electric drive components, NASA is looking to improve both the efficiency and the specific power of generators, motors, inverters, and rectifiers. A NASA research announcement has a goal of developing technologies and demonstrating an MW-class motor with efficiency greater than 96 percent and power density of greater than 13 kW/kg. This is just one component of the electric drive system. The partially turboelectric STARC-ABL (single-aisle turboelectric aircraft with aft boundary layer propulsor) aircraft concept assumes those values for the motors and generators, as well as rectifiers and inverters with 19 kW/kg and 99 percent efficiency. Stacking up all the components for this aircraft – including cables, circuit protection, and thermal management – yields an electric drive efficiency of 89.1 percent [7].

With regard to batteries, current state-of-the-art lithium-ion batteries have a specific energy on the cell level of up to 200 Wh/kg. Projected values in 15 and 30 years are 650 and 750 Wh/kg, respectively, for lithium–sulfur (LiS), and 950 and 1,400 Wh/kg, respectively, for lithium–air (Li-Air) [8]. These values have to be de-rated based on depth of discharge, battery structure, and battery management. For comparison, the specific energy of aviation fuel is approximately 12,000 Wh/kg.

Clearly, the benefits of improved propulsive efficiency from high BPR and BLI, as well as increased  $L/D$ , must be greater than the costs of electrified aircraft propulsion, and the balance of these benefits and constraints are presented here.

### 1.1.3 Aircraft Concepts with Electrified Propulsion

NASA has been investigating several different EAP systems for aircraft, including fully turboelectric, partially turboelectric, and parallel hybrid electric systems.

The N3-X concept shown in Figure 1.1 is a 300-passenger, HWB aircraft with a fully turboelectric propulsion system and a design range of 7,500 nautical miles (NM).

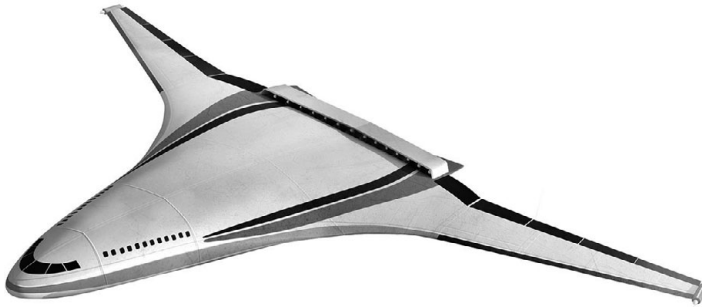


**Figure 1.1** N3-X concept vehicle.



**Figure 1.2** STARC-ABL concept vehicle.

Turbine engines are located at the wing tips, powering generators. Electric power is then transmitted through cables to a series of motor-driven fans located near the trailing edge of the aircraft. This configuration allows for a higher lift-to-drag ratio due to the hybrid wing body, as well as higher propulsive efficiency due to the increase in fan bypass ratio and boundary layer ingestion. This concept, described by Felder et al. [5], was conceived as a future-generation aircraft to meet NASA's goal of 70 percent fuel burn reduction. Out of the 70 percent overall improvements, 18–20 percent of fuel burn reduction was attributed to the turboelectric propulsion system architecture.

Figure 1.2 shows the partially turboelectric concept STARC-ABL, which is a 154-passenger aircraft with a design range of 3,500 NM. This commercial transport concept was developed for notional entry into service in 2035 and was compared to a conventional configuration using similar technology by Welstead and Felder [9]. The propulsion system consists of two underwing turbofans with generators extracting power from the fan shaft and transmitting it to a rear fuselage, axisymmetric, boundary layer ingesting fan. The power to the tailcone fan is constant and contributes approximately 20 percent of the thrust at takeoff and about 45 percent of the thrust at cruise. Analysis in [9] indicates that the partially turboelectric concept has an economic mission fuel burn reduction of 7 percent, and a design mission fuel burn reduction of 12 percent compared to the conventional configuration. It should be noted that subsequent studies have



**Figure 1.3** PEGASUS concept vehicle.

predicted fuel burn reductions that are in the range of 3–4 percent, but they were not available for referencing at the time of this publication.

The Parallel Electric-Gas Architecture with Synergistic Utilization Scheme (PEGASUS) concept is shown in Figure 1.3, which is a 48-passenger parallel hybrid electric aircraft. This concept is described by Antcliff and Capristan [10]. A detailed analysis of an intermediate parallel hybrid electric concept was performed by Antcliff et al. [11], which was based on the ATR-42-500 conventional fuel-based aircraft with a range of 600 NM. The analysis included various levels of battery specific energy, which is a critical parameter as battery weight has been shown to be a significant penalty for these types of aircraft. They found that a specific energy of 750 Wh/kg was required to break even on total energy, even as the aircraft weight increased over the baseline value.

The N3-X, STARC-ABL, and PEGASUS concepts will be used as case studies for the breakeven analysis in this study.

## 1.2 Breakeven Analysis

### 1.2.1 Key Performance Parameters and Key Assumptions

In order to conduct the breakeven analysis, we first define the key performance parameters (KPPs), the key assumptions, and the electrical power system boundary. Then we will formulate range equations for each aircraft type. Finally, we find the breakeven relationship by implicitly solving for the electric drive specific power and efficiency while holding constant the ratio of operating empty weight to initial weight, payload weight, input energy (from fuel and/or batteries), and aircraft flight range. The resulting parametric curves can be used as the top-level requirements for the electrical power system and bounding guidelines for further aircraft exploration.

Specifically, the key performance parameters (KPPs) are as follows:

- Electric drive system efficiency  $\eta_{\text{elec}}$ , expressed as a percentage.
- Electric drive system specific power  $Sp_{\text{elec}}$ , in kW/kg.
- Electric propulsion fraction  $\zeta$  for partially turboelectric and parallel hybrid electric aircraft.

The breakeven assumptions in this analysis used to determine the values of the KPPs include the following:

- The ranges of the conventional and electrified aircraft are equal.
- The input energy (fuel and/or battery energy) of the conventional and electrified aircraft are equal.
- The payload weights of all the aircraft are equal.
- The ratios of operating empty weights (OEW) to initial aircraft weights are equal, where OEW does not include the weights of the electric drive and batteries.

## 1.2.2 Electrified Aircraft Propulsion System Definitions

Each EAP system will now be described, along with the boundaries of the electric drive system for each case. In Figures 1.4–1.7 are shown simplified diagrams of the conventional (fuel-based) turbofan, fully turboelectric, partially turboelectric, and parallel hybrid electric aircraft propulsion systems, respectively. The conventional turbofan system is considered the baseline aircraft system for comparison. The building blocks of the systems are the energy source (fuel and/or battery), the turbine engine, the propulsor, and the electric drive for the EAP cases. We denote the *conventional turbofan aircraft*, *fully turboelectric*, *partially turboelectric*, and *parallel hybrid electric* parameters with the subscripts *AC*, *TE*, and *PE*, and *HE*, respectively. *Power* is denoted by the letter *P*, *efficiency* by  $\eta$ , *specific energy* by *Se*, and *specific power* by *Sp*.

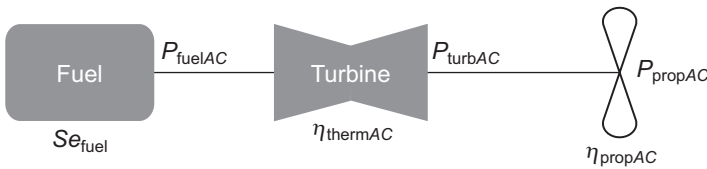


**Figure 1.4** Conventional, fuel-based aircraft propulsion system (AC).

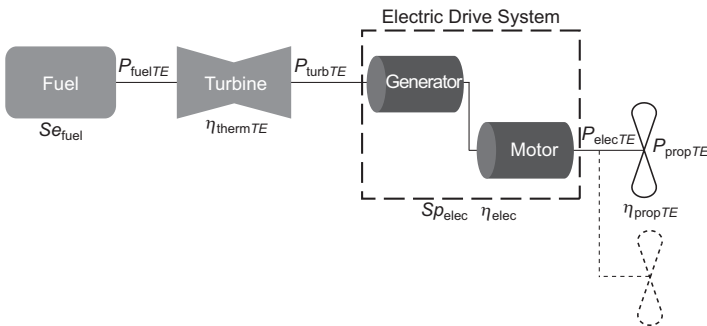


**Figure 1.5** Fully turboelectric aircraft propulsion system (TE).

The turbine, propulsor, and electric drive have associated thermal ( $\eta_{\text{therm}}$ ), propulsive ( $\eta_{\text{prop}}$ ), and electrical ( $\eta_{\text{elec}}$ ) efficiencies, expressed throughout this chapter as percentages. The fuel power  $P_{\text{fuel}}$ , battery power  $P_{\text{batt}}$ , turbine engine power  $P_{\text{turb}}$ , electrical power  $P_{\text{elec}}$ , and propulsive power  $P_{\text{prop}}$ , all in kW, are defined as output power of the fuel, battery, turbine engine, electric drive, and propulsors, respectively. The variables in Figures 1.4–1.7 illustrate the association between the propulsive subsystems, powers, and efficiencies for each propulsion system. In the partially turboelectric and parallel hybrid electric cases, we must introduce the electrical propulsion fraction  $\xi$ , defined as the fraction of total aircraft thrust at cruise produced by electrically driven propulsors. When the electrical propulsion fraction is equal to one, all the thrust during cruise is provided by electrically driven propulsors. The fully turboelectric system is one in which all the thrust throughout the mission, including takeoff and cruise, is provided by electrically driven propulsors. Therefore, the electric drive system will need to be sized accordingly.

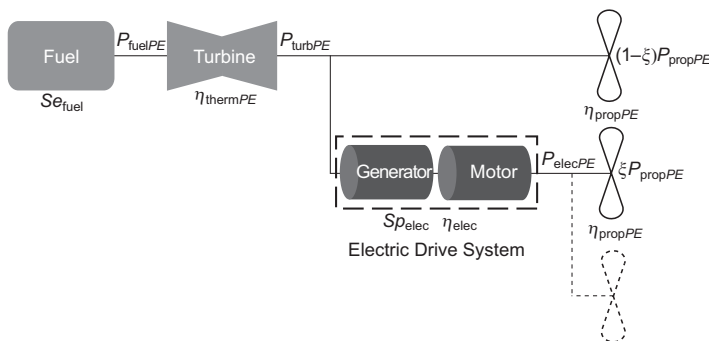


**Figure 1.6** Partially turboelectric aircraft propulsion system (PE).

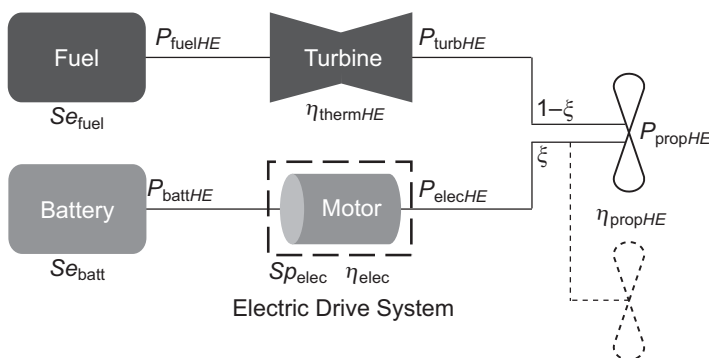


**Figure 1.7** Parallel hybrid electric propulsion system (HE).

The electric drive specific power, efficiency, and electrical propulsion fraction are the electrified aircraft electric drive system KPPs. Specific power is the ratio of the rated electric drive output power to its mass. Efficiency is the ratio of the output power to the input power of the electric drive system, multiplied by 100 percent. Electrical propulsion fraction is the fraction of total aircraft thrust at cruise produced by electrically driven propulsors. These three KPPs will be used to describe electrical power system performance and establish necessary levels of performance.

The boundary of the electric drive system is defined to lend meaning to the KPPs. In the analysis presented here, the boundary will include generators, rectifiers, distribution wiring, fault protection, inverters, motors, and the thermal control for those components. The parallel hybrid electric system does not require generators. Some variants of the electrical drive system may use a subset of these components or alternative layouts. The specific power and electrical efficiency analyzed in this study include all of the components inside the boundary. Notably, the turbine engine and the propulsors are outside the electric drive boundary.

A simplified assessment of the relationship of the electric drive system KPPs, aircraft range, and input energy is proposed for top-level aircraft performance comparisons. The range equations are discussed first, followed by the input energy, and, finally, the component weights. The breakeven equations are derived for fully turboelectric, partially turboelectric, and parallel hybrid electric aircraft.

### 1.2.3 Breakeven on Range

The basis of the analysis is an expansion of the traditional terms in the Breguet range equation for fuel-based aircraft to include the efficiency and weight of the electric drive system. The range equation for battery-powered aircraft from Hepperle [12] is expanded in a similar way. These equations apply to situations where overall aerodynamic efficiency,  $L/D$ , and flight velocity are constant over the duration of cruise. Although this is not true for the entire flight envelope, this description is a reasonable approximation for cruise conditions.

We develop range equations of the typical form, representing the conventional and EAP aircraft configurations concurrently for comparison. The range equations for fuel-based and battery-based aircraft are, respectively,

$$R_{\text{fuel}} = \frac{Se_{\text{fuel}} L}{g D} \eta_o \ln \left( \frac{W_i}{W_f} \right) \quad (1.1)$$

and

$$R_{\text{batt}} = \frac{Se_{\text{batt}} L}{g D} \eta_o \left( \frac{W_{\text{batt}}}{W_i} \right), \quad (1.2)$$

where  $R$  is the range, in m;  $Se_{\text{fuel}}$  and  $Se_{\text{batt}}$  are the specific energies of the fuel and battery, respectively, in J/Kg; and  $\eta_o$  is the overall efficiency percentage of the propulsion system.



For fuel-based aircraft, the final aircraft weight,  $W_f$ , is equal to the initial aircraft weight,  $W_i$ , minus the fuel weight,  $W_{\text{fuel}}$ , where all are expressed in N. Thus, the fuel-based range equation is

$$R_{\text{fuel}} = \frac{Se_{\text{fuel}} L}{g D} \eta_o \ln \left( \frac{1}{1 - W_{\text{fuel}}/W_i} \right). \quad (1.3)$$

Note that for small values of  $W_{\text{fuel}}/W_i$ ,

$$\ln \left( \frac{1}{1 - W_{\text{fuel}}/W_i} \right) \approx \frac{W_{\text{fuel}}}{W_i}, \quad (1.4)$$

which shows that Equations (1.1) and (1.2) have a similar form. Thus, the range is approximately proportional to the ratio of the energy source weight to the aircraft initial weight. Since  $Se_{\text{batt}} \ll Se_{\text{fuel}}$ , battery weight for the same range will be much larger than fuel weight.

The overall efficiency of each aircraft type is defined in Equations (1.5)–(1.8) in Table 1.1 as functions of propulsive, thermal, and electric drive efficiency. Note that the propulsive efficiency defined here is actually the product of transfer efficiency and propulsive efficiency.

To see how adding the electric drive system affects overall efficiency, the ratio of electrified aircraft to baseline conventional overall efficiency is plotted in Figure 1.8 as a function of electric propulsion fraction. Here it is assumed that the thermal efficiency is 55 percent and the electric drive efficiency is 90 percent. Increasing  $\xi$  decreases overall efficiency for the turboelectric cases, since the electric drive system is in series with the turbine engine. Since  $\eta_{\text{elec}}$  is larger than  $\eta_{\text{therm}}$ , the hybrid electric system has increasing overall efficiency compared to the baseline. However, the battery weight required for hybrid electric will be a significant penalty in the breakeven analysis.

## 1.2.4 Breakeven on Input Energy

The input energy of fuel is simply the product of the specific energy of the fuel and the fuel mass. Similarly, the input energy of the battery is simply the product

**Table 1.1** Overall efficiency equations.

Aircraft type	Overall efficiency
Conventional aircraft (AC)	$\eta_{oAC} = \eta_{\text{prop}AC} \times \eta_{\text{therm}AC}$ (1.5)
Fully turboelectric aircraft (TE)	$\eta_{oTE} = \eta_{\text{prop}TE} \times \eta_{\text{therm}TE} \times \eta_{\text{elec}TE}$ (1.6)
Partially turboelectric aircraft (PE)	$\eta_{oPE} = \frac{\eta_{\text{prop}PE} \times \eta_{\text{therm}PE} \times \eta_{\text{elec}PE}}{(1 - \xi)\eta_{\text{elec}PE} + \xi}$ (1.7)
Parallel hybrid electric aircraft (HE)	$\eta_{oHE} = \frac{\eta_{\text{prop}HE} \times \eta_{\text{therm}HE} \times \eta_{\text{elec}HE}}{(1 - \xi)\eta_{\text{elec}HE} + \xi\eta_{\text{therm}HE}}$ (1.8)

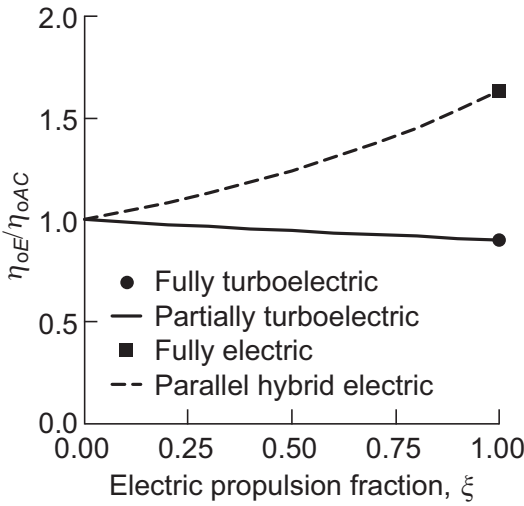


Figure 1.8 Ratio of electrified to conventional aircraft overall efficiency.

of the specific energy of the battery and the battery mass. Thus, the input energy equations are

$$E_{fuel} = \frac{Se_{fuel}}{g} W_{fuel} \tag{1.9}$$

and

$$E_{batt} = \frac{Se_{batt}}{g} W_{batt}. \tag{1.10}$$

### 1.2.5 Relationship among Aircraft Component Weights

The final part of the breakeven analysis relates the specific power of the EAP system to the other component weights. We know that the initial aircraft weight is defined as the sum of the OEW, payload weight, fuel weight, electric drive system weight (for electrified aircraft), and battery weight (for HE aircraft):

$$W_i = W_{OEW} + W_{payload} + W_{fuel} + W_{elec} + W_{batt}. \tag{1.11}$$

From Equation (1.11) we can see that

$$\frac{W_{elec}}{W_i} = 1 - \frac{W_{OEW}}{W_i} - \frac{W_{fuel}}{W_i} - \frac{W_{batt}}{W_i} - \frac{W_{payload}}{W_i}, \tag{1.12}$$

noting that the payload weight and the ratio of OEW to initial aircraft weight are constant among the aircraft.

For the TE aircraft, where all the power must pass through the electric drive system,  $Sp_{elec}$  will be defined based on takeoff power rather than cruise power.

If we denote the ratio of takeoff to cruise power as  $\alpha$ , then the electric drive system weight ratio is [1]

$$\frac{W_{\text{elecTE}}}{W_{\text{iTE}}} = \frac{\alpha v_{\text{cruise}}}{\left(\frac{L}{D}\eta_{\text{prop}}\right)_{\text{TE}} Sp_{\text{elec}}/g}. \quad (1.13)$$

Alternatively, it is assumed for the partially turboelectric and parallel hybrid electric cases that electric propulsion power, which is the product of  $\zeta$  and propulsion power, is not required for takeoff, so the electric drive system weight ratio is defined as [2]

$$\frac{W_{\text{elecHE,PE}}}{W_{\text{iHE,TE}}} = \frac{\zeta v_{\text{cruise}}}{\left(\frac{L}{D}\eta_{\text{prop}}\right)_{\text{HE,PE}} Sp_{\text{elec}}/g}. \quad (1.14)$$

## 1.3 Breakeven Results

### 1.3.1 Fully Turboelectric Aircraft (TE)

Equations for the fully turboelectric aircraft for the range, input energy, and component weight equations, respectively, are as follows:

$$\ln\left(1 - \frac{W_{\text{fuelTE}}}{W_{\text{iTE}}}\right) = \frac{\left(\frac{L}{D}\eta_{\text{prop}}\eta_{\text{therm}}\right)_{\text{AC}}}{\left(\frac{L}{D}\eta_{\text{prop}}\eta_{\text{therm}}\eta_{\text{elec}}\right)_{\text{TE}}} \ln\left(1 - \frac{W_{\text{fuelAC}}}{W_{\text{iAC}}}\right) \quad (1.15)$$

$$\frac{W_{\text{iAC}}}{W_{\text{iTE}}} = \frac{\left(\frac{W_{\text{fuelTE}}}{W_{\text{iTE}}}\right)}{\left(\frac{W_{\text{fuelAC}}}{W_{\text{iAC}}}\right)} \quad (1.16)$$

and

$$\frac{W_{\text{elecTE}}}{W_{\text{iTE}}} = \left(1 - \frac{W_{\text{fuelTE}}}{W_{\text{iTE}}} - \frac{W_{\text{OEW}}}{W_{\text{i}}}\right) - \frac{W_{\text{iAC}}}{W_{\text{iTE}}} \left(1 - \frac{W_{\text{fuelAC}}}{W_{\text{iAC}}} - \frac{W_{\text{OEW}}}{W_{\text{i}}}\right). \quad (1.17)$$

Several observations can be made from Equations (1.15) to (1.17). First, Equation (1.15) shows that the fuel fraction for the turboelectric aircraft will be reduced if the product of  $L/D$  and overall efficiency is increased compared to the baseline aircraft. Then Equation (1.16) shows that the aircraft weight will increase compared to the baseline, which is a result of the added electric drive system.

To solve this set of equations for  $Sp_{\text{elec}}$ , we first assume a value of  $\eta_{\text{elec}}$  (e.g.,  $\eta_{\text{elec}} = 100$  percent). Equation (1.15) then yields the fuel fraction  $W_{\text{fuelTE}}/W_{\text{iTE}}$ , given the baseline fuel fraction and assumed values for  $L/D$  and  $\eta$ . From Equation (1.16), we find the ratio of conventional initial aircraft weight to turboelectric initial aircraft weight, which is then substituted Equation (1.17) to give the electric drive system weight ratio  $W_{\text{elecTE}}/W_{\text{iTE}}$ . Finally, Equation (1.13) is solved for  $Sp_{\text{elec}}$ . This is

repeated for a range of values of  $\eta_{elec}$ , resulting in a curve of  $\eta_{elec}$  vs.  $Sp_{elec}$  for the turboelectric system. This procedure is used in a similar way for the partially turboelectric and parallel hybrid electric propulsion systems, using the appropriate equations for those aircraft.

Similar to the results given by Jansen et al. [1], the electric drive specific power and efficiency required to break even on range and input energy were determined, based on expected propulsive improvements. Again, the difference between this analysis and the previous analysis is that the breakeven is based on constant input energy and constant ratio of OEW to initial weight in this study, whereas it is based on constant initial weight and OEW in the previous study.

The turboelectric aircraft studied here is based on the NASA N3-X hybrid wing body fully turboelectric aircraft. In Felder et al. [5], the N3-X was compared to two different baseline aircraft configurations – a conventional tube-and-wing aircraft (a Boeing 777-200 LR) and an intermediate hybrid wing body aircraft with conventional propulsion (a NASA N3A concept). Table 1.2 details the parameters used in the analysis. For all the aircraft, it is assumed that the transfer efficiency is 80 percent (which is multiplied by the propulsive efficiency supplied in the study to give  $\eta_{prop}$ ), and the thermal efficiency  $\eta_{therm}$  is assumed to be 55 percent.

First, we look at the effect of aero and propulsive benefits on the breakeven curves. Here the baseline parameters  $\eta_{prop}$  and  $L/D$  are based on the Boeing 777 aircraft, and the maximum benefits are those for the fully turboelectric N3-X aircraft. We look at three benefit levels between the baseline 777 and N3-X; these include combined aero and propulsive benefits of 7, 18, and 29 percent for minimum, medium, and maximum benefits, respectively. The 29 percent benefit is representative of the N3-X versus the 777 baseline with the  $L/D$  and  $\eta_{prop}$  improvements shown in Table 1.2.

The breakeven curves for the three levels of propulsive benefits are shown in Figure 1.9. Electric drive systems with performance above each curve should result in lower fuel burn. Clearly, improving  $L/D$  and  $\eta_{prop}$  leads to lower demands on the electric drive system. Table 1.2 includes the specific power and efficiency expected of a superconducting electric drive system, 7.1 kW/kg and 98.54 percent. With these values, only the medium and maximum benefits case would result in lower fuel burn.

**Table 1.2** Fully turboelectric aircraft parameters.

Parameter	Baseline 777	Baseline N3A	Turboelectric N3-X
$\alpha$	2.0	1.8	
$v_{cruise}$ [m/s]	255	255	255
$W_{fuelAC}/W_{iAC}$	36%	24%	
$W_{OEW}/W_i$	48%	54%	48%/54%
$L/D$	19	22	22
$\eta_{prop}$	69.6%	72.2%	77.1%
$Sp_{elec}$ [kW/kg]			7.1
$\eta_{elec}$			98.54%

Relaxing the efficiency to 90 percent, as for a non-superconducting electric drive system, only the maximum benefits case would result in lower fuel burn.

The ratio of electric drive weight to initial turboelectric aircraft weight as a function of specific power is illustrated in Figure 1.10. Clearly, the higher the specific power is, the lighter the electric drive system will be. For the minimum allowable specific power of 3.1 kW/kg for maximum benefits at 100 percent efficiency, the electric drive system comprises 9.6 percent of the aircraft weight. This number quickly falls with increasing specific power.

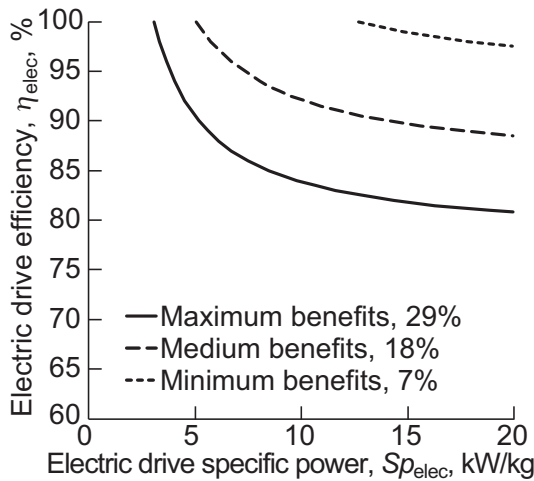


**Figure 1.9** Breakeven curves for turboelectric propulsion.

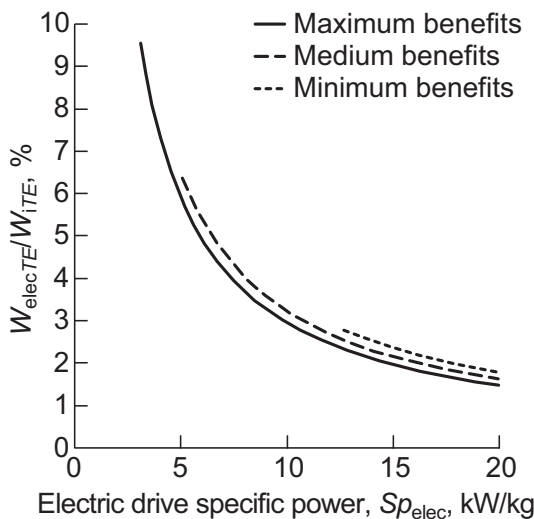


**Figure 1.10** Electric drive weight ratio for turboelectric propulsion.

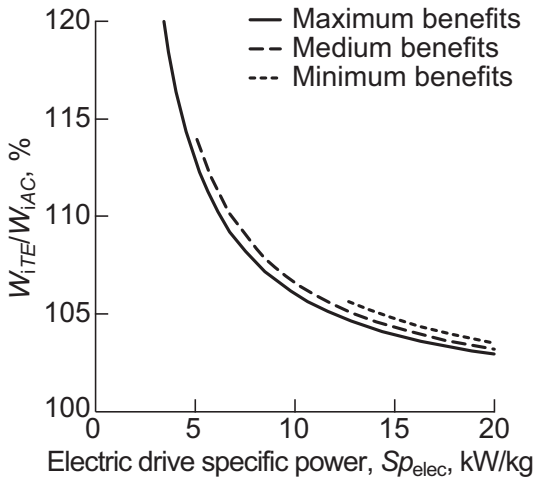


**Figure 1.11** Ratio of turboelectric to baseline aircraft weight in breakeven analysis.

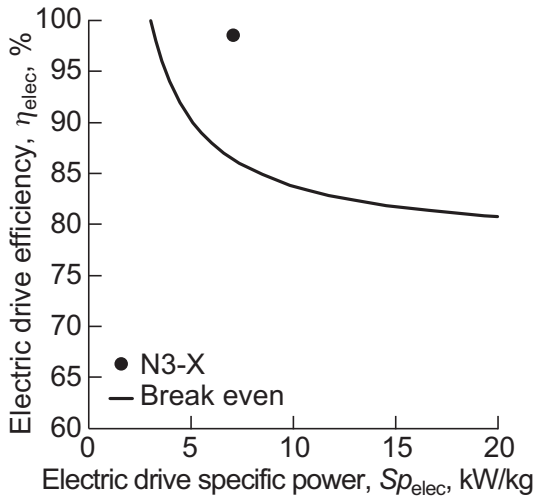


**Figure 1.12** Breakeven for N3-X vs. 777.

Finally, Figure 1.11 shows the increase in the turboelectric aircraft weight as a function of electric drive specific power. This particular breakeven analysis results in heavier aircraft, but with the same fuel burn as the baseline aircraft.

The electric drive breakeven curves for the turboelectric N3-X versus the baseline 777 and the baseline N3A, respectively, are shown in Figures 1.12 and 1.13. The electric drive efficiency and power indicated by the orange symbols is for a superconducting system, which has very high performance. In Figure 1.13, we see that the electric drive system used in the N3-X analysis does not provide fuel burn benefits in

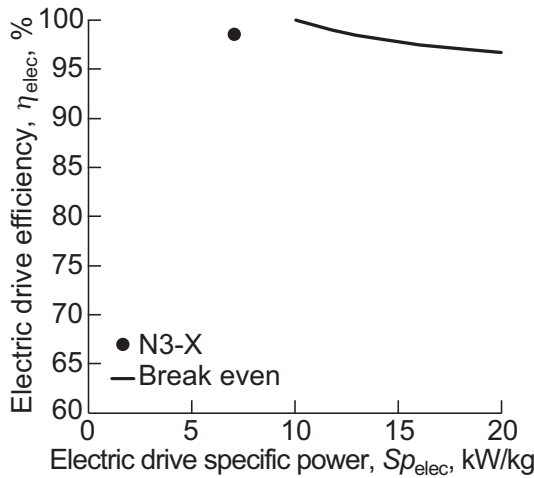


**Figure 1.13** Breakeven for N3-X vs. N3A.

this breakeven analysis, even though results in [5] indicate reduced fuel burn. The discrepancy lies in the breakeven analysis assumptions. Here we are assuming equal input power, which in this case is equal fuel burn. This results in a larger aircraft compared to the baseline N3A. However, the N3-X aircraft actually had a 7 percent lower aircraft weight than the baseline N3A. This illustrates the sensitivity of this breakeven analysis to the key assumptions. However, Figure 1.13 does clearly indicate the necessity of choosing the high-performance superconducting electric drive.

### 1.3.2 Partially Turboelectric Aircraft (PE)

Equations for the partially turboelectric aircraft for the range, input energy, and component weight equations, respectively, are as follows:

$$\ln\left(1 - \frac{W_{\text{fuelPE}}}{W_{iPE}}\right) = \frac{\left(\frac{L}{D}\eta_{\text{prop}}\eta_{\text{therm}}\right)_{AC}}{\left(\frac{L}{D}\eta_{\text{prop}}\eta_{\text{therm}}\eta_{\text{elec}}\right)_{PE}} \ln\left(1 - \frac{W_{\text{fuelAC}}}{W_{iAC}}\right) \quad (1.18)$$

$$\frac{W_{iAC}}{W_{iPE}} = \frac{\left(\frac{W_{\text{fuelPE}}}{W_{iPE}}\right)}{\left(\frac{W_{\text{fuelAC}}}{W_{iAC}}\right)} \quad (1.19)$$

and

$$\frac{W_{\text{elecPE}}}{W_{iPE}} = \left(1 - \frac{W_{\text{fuelPE}}}{W_{iPE}} - \frac{W_{\text{OEW}}}{W_i}\right) - \frac{W_{iAC}}{W_{iPE}} \left(1 - \frac{W_{\text{fuelAC}}}{W_{iAC}} - \frac{W_{\text{OEW}}}{W_i}\right). \quad (1.20)$$

**Table 1.3** Partially turboelectric aircraft parameters.

Parameter	Baseline N3CC	Partially turboelectric STARC-ABL
$\zeta$		45%
$v_{\text{cruise}}$ [m/s]	206	206
$W_{\text{fuelAC}}/W_{\text{iAC}}$	17%	
$W_{\text{OEW}}/W_{\text{i}}$	57%	57%
$L/D$	21.4	22.3
$\eta_{\text{prop}}$	64%	75.1%
$Sp_{\text{elec}}$ [kW/kg]		2.0
$\eta_{\text{elec}}$		90%

These equations are similar to the fully turboelectric case, except in the definitions of overall efficiency (Eqs. (1.7) vs. (1.6)) and electric drive system weight (Eqs. (1.14) vs. (1.13)).

The effect of electric propulsion fraction on required electric drive system performance was examined for the case of the partially turboelectric STARC-ABL aircraft concept. In [9], Welstead and Felder performed a systems study of the STARC-ABL aircraft compared to an N+3 Conventional Configuration (N3CC) baseline conventional fuel-powered turbofan aircraft. Table 1.3 shows the baseline and partially turboelectric aircraft parameters used in the breakeven analysis. The propulsive efficiency for a CFM56 fan is assumed to be 80 percent, which is multiplied by the transfer efficiency of 80 percent to give 64 percent. Similarly, the propulsive efficiency of 93.9 percent for the GE hFan is used for the STARC-ABL analysis and is multiplied by 80 percent to give 75.1 percent.

If we assume that  $L/D$  and  $\eta_{\text{prop}}$  are constant with changing electric propulsion fraction, then the breakeven curves are as shown in Figure 1.14. The STARC-ABL aircraft has an electric propulsion fraction  $\zeta$  of 45 percent at cruise, and if we assume that the aero and propulsive parameters  $L/D$  and  $\eta_{\text{prop}}$  for the STARC-ABL in Table 1.3 scale with  $\zeta$ , then the breakeven curves are as shown in Figure 1.15. This shows the effect of the benefits versus the costs of the electric drive system and the importance of predicting those benefits in this type of analysis.

In Figure 1.16 the electric drive weight ratio is shown, assuming constant  $\eta_{\text{prop}}$  and  $L/D$ . The weights are lower for partially turboelectric compared to the fully turboelectric, since the electric drive system is sized based on cruise power rather than takeoff power. The ratio of initial weights, comparing partially turboelectric aircraft to conventional aircraft, is plotted in Figure 1.17.

The results of the breakeven analysis for the STARC-ABL concept at its design electric propulsion fraction of 45 percent are plotted in Figure 1.18. Here we see that the electric drive efficiency and specific power used in [9] does result in an aircraft with lower fuel burn. Unlike the N3-X example, the STARC-ABL aircraft actually has a 3 percent higher initial weight than the baseline, whereas the breakeven analysis shows a 7 percent higher initial weight at  $Sp_{\text{elec}} = 2 \text{ kW/kg}$ .



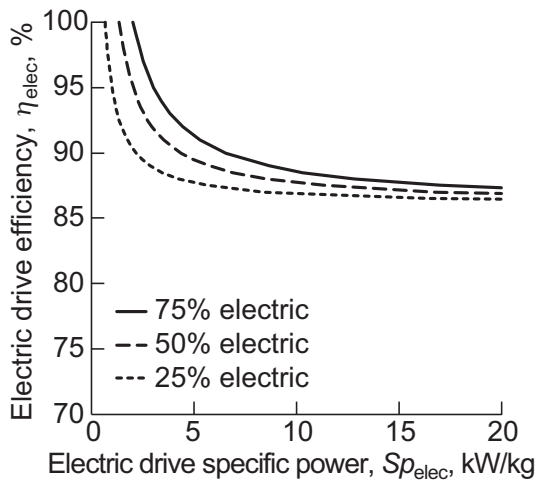


**Figure 1.14** Breakeven curves for partially turboelectric aircraft with constant aero and propulsive benefits.

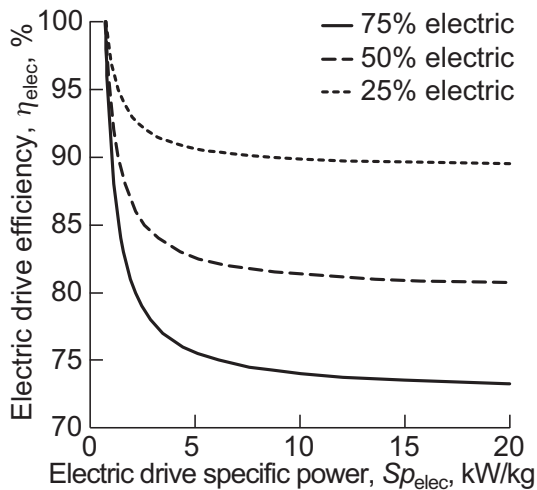


**Figure 1.15** Breakeven curves for partially turboelectric aircraft with scaled aero and propulsive benefits.

In general, the breakeven analysis assumptions are similar to the systems study in [9]; therefore, the results are similar.

### 1.3.3 Parallel Hybrid Electric Aircraft (HE)

Equations for the parallel hybrid electric aircraft for the fuel range, electrical propulsion fraction, input energy, and component weight equations, respectively, are as follows:

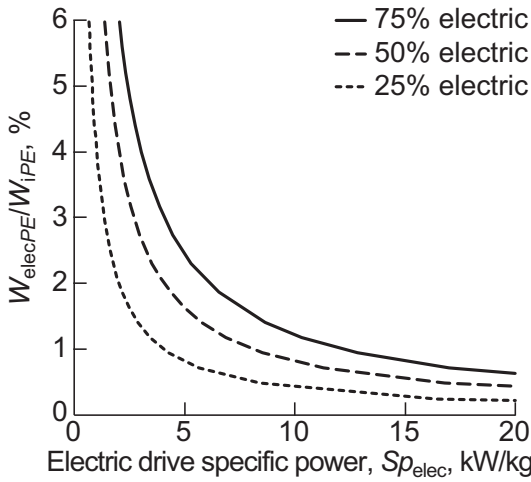


**Figure 1.16** Electric drive weight ratio for partially turboelectric aircraft with constant aero and propulsive benefits.

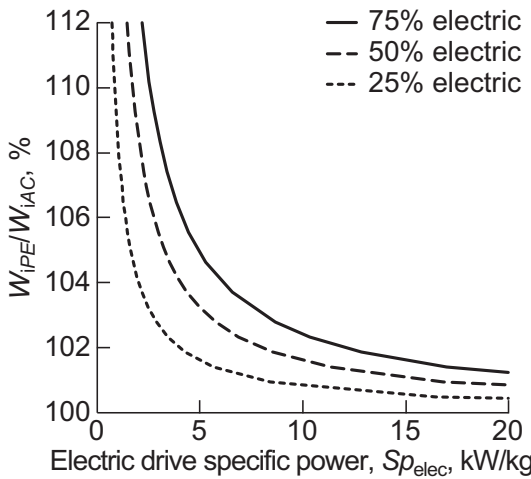


**Figure 1.17** Ratio of partially turboelectric to baseline aircraft weight with constant aero and propulsive benefits.

$$\ln \left( 1 - \frac{W_{fuelHE}}{W_{iHE}} \right) = (1 - \zeta) \frac{\left( \frac{L}{D} \eta_{prop} \eta_{therm} \right)_{AC}}{\left( \frac{L}{D} \eta_{prop} \eta_{therm} \right)_{HE}} \ln \left( 1 - \frac{W_{fuelAC}}{W_{iAC}} \right) \quad (1.21)$$

$$\frac{W_{battHE}}{W_{iHE}} = \left( \frac{\zeta}{1 - \zeta} \right) \frac{S_{e_{fuel}} \eta_{thermHE}}{S_{e_{batt}} \eta_{elecHE}} \frac{W_{fuelHE}}{W_{iHE}} \quad (1.22)$$

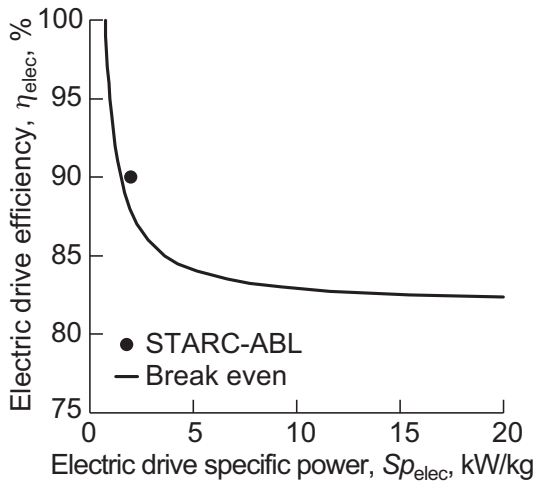


Figure 1.18 Breakeven for STARC-ABL vs. N3CC.

$$\frac{W_{iAC}}{W_{iHE}} = \frac{Se_{batt} \left( \frac{W_{battHE}}{W_{iHE}} \right) + Se_{fuel} \left( \frac{W_{fuelHE}}{W_{iHE}} \right)}{Se_{fuel} \left( \frac{W_{fuelAC}}{W_{iAC}} \right)} \quad (1.23)$$

And

$$\frac{W_{elecHE}}{W_{iHE}} = \left( 1 - \frac{W_{fuelHE}}{W_{iHE}} - \frac{W_{OEWE}}{W_i} - \frac{W_{battHE}}{W_{iHE}} \right) - \frac{W_{iAC}}{W_{iHE}} \left( 1 - \frac{W_{fuelAC}}{W_{iAC}} - \frac{W_{OEWE}}{W_i} \right). \quad (1.24)$$

The additional equation in this case, Equation (1.22), results from the assumption that the battery-powered portion of the thrust is defined by the electrical propulsion fraction,  $\zeta$ . We can see from Equation (1.22) that the ratio of battery weight to initial aircraft weight is directly proportional to the ratio of fuel specific energy to battery specific energy. The fuel specific energy is approximately 12,000 Wh/kg, compared to projected battery specific energy of 500, 750, or 1,000 Wh/kg. It is easy to see that the battery weight can become quite large, making hybrid electric configurations more difficult to implement than partially turboelectric configurations, despite the better overall efficiency. However, there are some conditions under which the hybrid electric configuration is more successful. To that end, we investigate the effect of range,  $Se_{batt}$ , and electric propulsion fraction  $\zeta$  on the breakeven curves.

A breakeven analysis was performed for the parallel hybrid electric aircraft described by Antcliff et al. [10, 11]. This is a short-range aircraft devised for 48 passengers; the shorter range makes it a better choice for hybrid electric. The baseline conventional aircraft is the ATR 42-500, which utilizes two turboprop engines. There is an intermediate parallel hybrid electric concept with a range of 600 NM and the

parameters shown in Table 1.4. Here the propulsive efficiencies are calculated assuming a transfer efficiency of 80 percent and  $\eta_{\text{therm}} = 55$  percent. The parallel hybrid electric PEGASUS concept has a 400 NM range, and a fully electric (at cruise) PEGASUS concept has a 200 NM range.

To start, the effect of aircraft range was examined. The aircraft range is approximately proportional to the baseline aircraft fuel fraction,  $W_{\text{fuelAC}}/W_{\text{iAC}}$ . Therefore, examining the effect of this fuel fraction in the breakeven analysis is essentially the same as examining the effect of the range. We looked at two values of baseline fuel fraction: 0.05 (shorter range) and 0.091 (baseline 600 NM). Compared to the aircraft in the turboelectric and partially turboelectric studies, this range is quite small. Figure 1.19 shows the electric drive performance required for the two ranges for  $S_{e\text{batt}} = 750$  Wh/kg and  $\zeta = 25$  percent. Clearly, the parallel hybrid electric

**Table 1.4** Parallel hybrid electric aircraft parameters.

Parameter	Baseline	Parallel hybrid electric
$\zeta$		25%, 50%, 75%
$v_{\text{cruise}}$ [m/s]	150	150
$W_{\text{fuelAC}}/W_{\text{iAC}}$	9.1%	
$W_{\text{OEW}}/W_{\text{i}}$	64%	64%
$L/D$	11	15
$\eta_{\text{prop}}$	60%	72%
$S_{e\text{batt}}$ [Wh/kg]		500, 750, 1,000
$S_{p\text{elec}}$ [kW/kg]		7.3
$\eta_{\text{elec}}$		90%

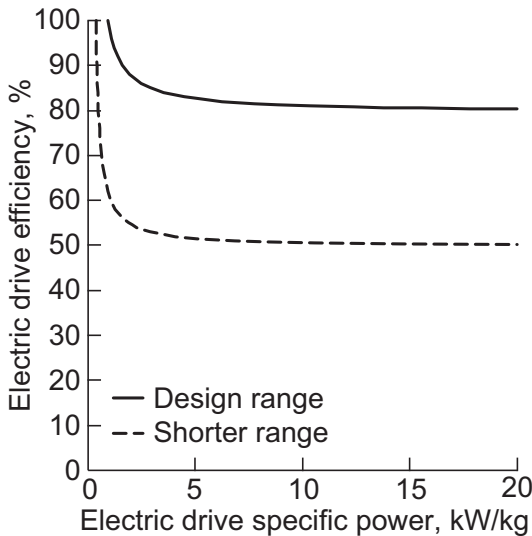


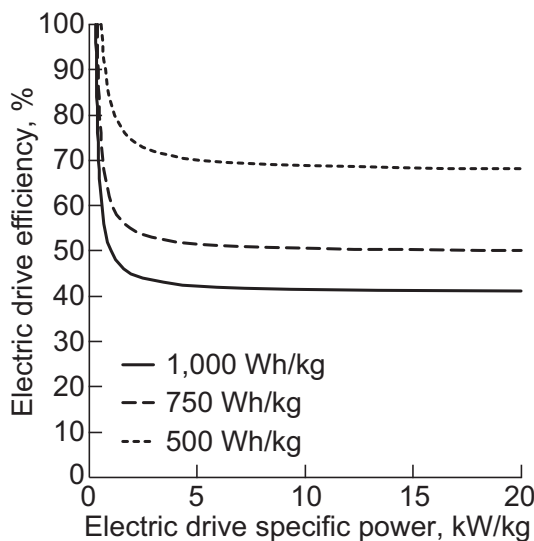
**Figure 1.19** Breakeven curves based on aircraft range,  $\zeta = 25$  percent,  $S_{e\text{batt}} = 750$  Wh/kg.

configuration is a better option for shorter range flights, which is expected. Note that the electrical efficiency required for the shorter-range flight is very low. This is a result of the parallel configuration. For constant  $\eta_{\text{therm}}$ , as long as  $(\eta_{\text{elec}}\eta_{\text{prop}})_{\text{HE}} > (\eta_{\text{therm}}\eta_{\text{prop}})_{\text{AC}}$ , the overall efficiency will be higher than the baseline. There are certainly weight penalties, especially for the battery weight, but these can be overcome depending on the aero and propulsive benefits, which are quite high for this case.

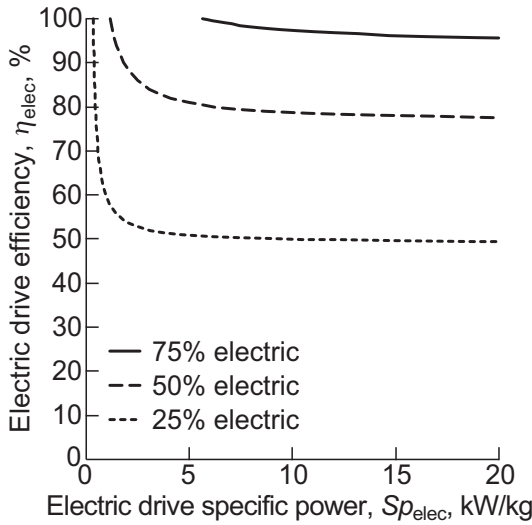
Next, the effect of battery specific energy was examined for the shorter range  $W_{\text{fuelAC}}/W_{\text{iAC}} = 0.05$ . The results for  $\zeta = 25$  percent for  $S_{e_{\text{batt}}} = 500, 750,$  and  $1,000$  Wh/kg are given in Figure 1.20. As expected, carrying the heavier batteries increases the performance required of the electric drive system.

Figure 1.21 shows the breakeven curves for various values of electric propulsion fraction for  $W_{\text{fuelAC}}/W_{\text{iAC}} = 0.05$  and  $S_{e_{\text{batt}}} = 750$  Wh/kg, assuming the aero and propulsive benefits are constant. If we assume that these  $\eta_{\text{prop}}$  and  $L/D$  change with  $\zeta$ , normalizing the benefits to  $\zeta = 50$  percent, then the breakeven curves are as shown in Figure 1.22. There is a big difference between the two charts, and it clearly illustrates the balance between the aero and propulsive benefits and the costs of the battery and electric drive system.

Returning to the assumption that the aero and propulsive benefits remain constant, Figures 1.23–1.25, respectively, show the electric drive weight fraction, the battery weight fraction, and the ratio of hybrid electric aircraft weight to conventional aircraft initial weight. Compared to the fully and partially turboelectric aircraft, the hybrid electric aircraft requires significant added weight.



**Figure 1.20** Breakeven curves based on battery specific energy,  $\zeta = 25$  percent,  $W_{\text{fuelAC}}/W_{\text{iAC}} = 0.05$ .



**Figure 1.21** Breakeven curves based on electric propulsion fraction with aero and propulsive benefits constant,  $S_{e_{batt}} = 750$  Wh/kg, and  $W_{fuel_{AC}}/W_{i_{AC}} = 0.05$ .

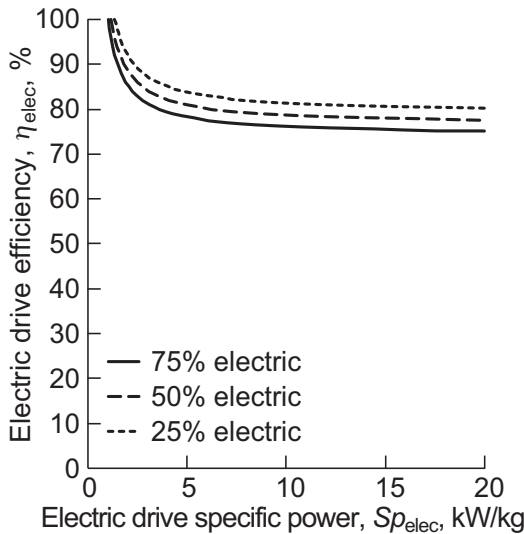


**Figure 1.22** Breakeven curves based on electric propulsion fraction with aero and propulsive benefits scaling with  $\zeta$ ,  $S_{e_{batt}} = 750$  Wh/kg, and  $W_{fuel_{AC}}/W_{i_{AC}} = 0.05$ .

Now we look at the 600 NM range parallel hybrid electric aircraft described in Table 1.4, with a fuel fraction of 0.091. We compare breakeven results with those found in [11], which show that the 750 Wh/kg battery approximately breaks even on input power. This is one of our analysis assumptions, making it a good study for

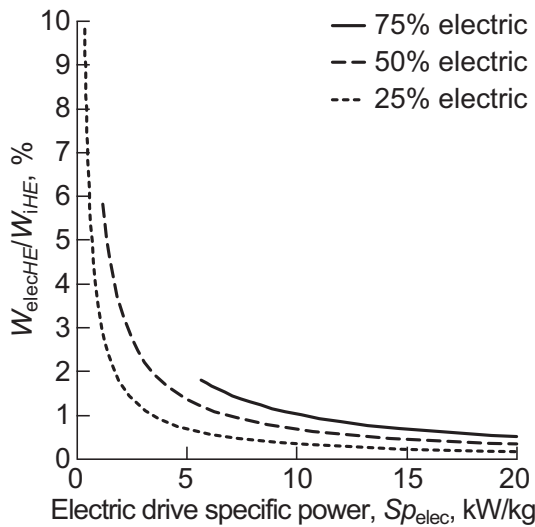


**Figure 1.23** Electric drive weight ratio with equal benefits,  $Se_{\text{batt}} = 750 \text{ Wh/kg}$ , and  $W_{\text{fuelAC}}/W_{\text{iAC}} = 0.05$ .

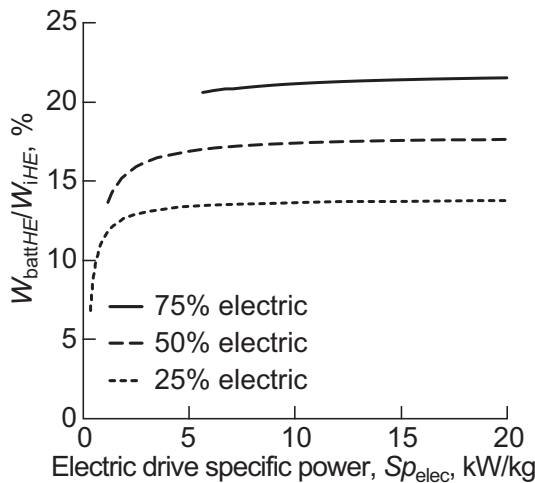


**Figure 1.24** Battery weight ratio with equal benefits,  $Se_{\text{batt}} = 750 \text{ Wh/kg}$ , and  $W_{\text{fuelAC}}/W_{\text{iAC}} = 0.05$ .

comparison. The 500 Wh/kg battery increases total energy, and the 1,000 Wh/kg battery decreases total energy.

Figure 1.26 shows the results for the parallel hybrid electric concept in our breakeven analysis for an electric propulsion fraction of 25 percent. As expected, the 750 Wh/kg battery breakeven line was relatively close to the electric drive efficiency and specific power used in the systems study, which found nearly equal

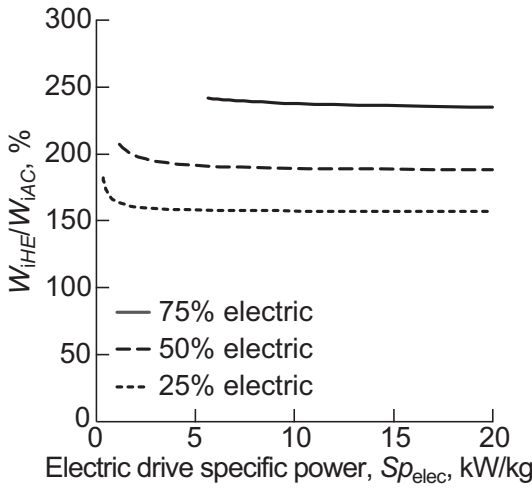


**Figure 1.25** Ratio of hybrid electric aircraft weight to conventional aircraft weight with equal benefits,  $Se_{batt} = 750 \text{ Wh/kg}$ , and  $W_{fuel_{AC}}/W_{i_{AC}} = 0.05$ .

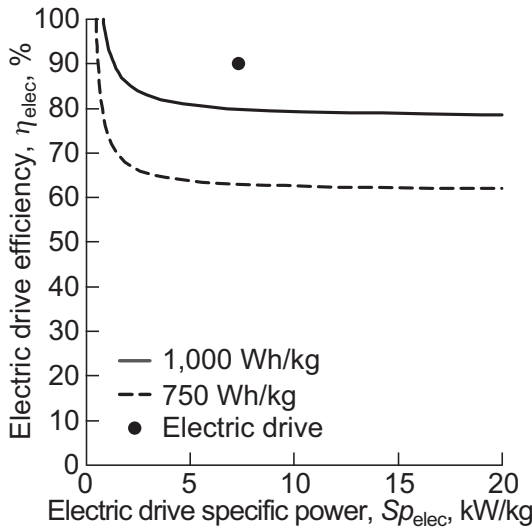


**Figure 1.26** Breakeven for parallel hybrid electric aircraft example at  $\zeta = 25$  percent.

input power for that configuration. Improving  $Se_{batt}$  to 1,000 Wh/kg allows a relaxation in the electric drive performance. The breakeven analysis did not yield any viable electric drive performance for the 500 Wh/kg battery, as expected.

These results look good; however, increasing the electric propulsion fraction to 50 percent or higher does not yield feasible electric drive properties in this breakeven analysis, while in [11] the authors did find viable configurations. Further inspection of



those results reveals that the assumption of  $W_{\text{OEW}}/W_i$  remaining constant is not true for that study. We made an assumption that the aircraft would need to be sized up to carry the weight of the added batteries. If the assumption is made that  $W_{\text{OEW}}/(W_i - W_{\text{batt}})$  remains constant, which is similar to the Antcliff results, then viable electric drive configurations can be found for  $\xi > 25$  percent.

## 1.4 Summary

The electrified aircraft propulsion concepts for commercial transport aircraft include a very wide range of propulsion airframe integration options as well as electric drive train options. Bounding analyses or parametric trade studies can be very useful to help narrow choices for detailed studies as well as guide technology development choices. Specific power, efficiency, and electric propulsion fraction have been proposed as KPPs for the electric drive system of an electrified aircraft. The boundary of the system is defined between the output shafts of the turbine to the input shaft of the propulsor and includes the electrical machines, power distribution, any other power components related to propulsion, as well as any thermal systems associated with the power system. Equations were developed that compare the benefits and costs of an electrified aircraft propulsion system compared to the baseline conventional aircraft. Some key conclusions include the following:

- Fully turboelectric aircraft
  - The electric drive system must provide power for takeoff results in tougher requirements on specific power than for partially turboelectric aircraft.
- Partially turboelectric aircraft
  - Assuming constant aero and propulsive benefits, a higher electric propulsion fraction requires a better performing electric drive system, due to the added weight of the electric drive system.
  - Assuming propulsive benefits that scale with electric propulsion fraction, a higher electric propulsion fraction relaxes the requirements of the electric drive system, since the higher aero and propulsive benefits cancel the costs of the electric drive system.
- Parallel hybrid electric aircraft
  - Parallel hybrid electric aircraft is better suited to shorter range.
  - Improving battery specific energy will make hybrid electric configurations more feasible.
  - Assuming constant aero and propulsive benefits, increasing the electric propulsion fraction increases the demands on the electric drive system to an even larger extent than the partially turboelectric system because of the added battery weight.
  - Assuming propulsive benefits that scale with electric propulsion fraction, a higher electric propulsion fraction relaxes the requirements of the electric drive system. Again, the higher aero and propulsive benefits cancel the costs of the

electric drive system. However, the added battery weight makes the benefits less dramatic compared to the partially turboelectric system.

- All electric aircraft
  - The breakeven curves are very sensitive to the propulsive benefit assumptions.
  - The breakeven analysis is sensitive to the component weight assumptions. Here it was assumed that the ratio of OEW to initial aircraft weight remains constant. It may be that other component assumptions are better for a given configuration, which could easily be incorporated into the breakeven analysis.
  - In general, at low specific power, the efficiency of the electric drive system dominates. But increasing specific power above a certain level yields diminishing returns.

## Abbreviations

AC	conventional, fuel-based aircraft propulsion system (used as a subscript)
AFPM	axial flux permanent magnet
BLI	boundary layer ingestion
BPR	bypass ratio
EAP	electrified aircraft propulsion
HE	parallel hybrid electric propulsion system (used as a subscript)
HWB	hybrid wing body
KPP	key performance parameter
$L/D$	lift-to-drag ratio
LiAir	lithium-air
LiS	lithium-sulfur
N3CC	N+3 conventional configuration
NASA	National Aeronautics and Space Administration
NM	nautical mile
OEW	operating empty weight
PE	partially turboelectric aircraft propulsion system (used as a subscript)
PEGASUS	Parallel Electric-Gas Architecture with Synergistic Utilization Scheme
STARC-ABL	single-aisle turboelectric aircraft with aft boundary layer propulsor
TE	fully turboelectric aircraft propulsion system (used as a subscript)

## Variables

$D$	drag, [N]
$g$	acceleration due to gravity on Earth, [9.81 m/s <sup>2</sup> ]
$E_{\text{batt}}$	input energy of battery-based aircraft, [J]

$E_{\text{fuel}}$	input energy of fuel-based aircraft, [J]
$L$	lift, [N]
$P_{\text{batt}}$	battery output power, [kW]
$P_{\text{elec}}$	electrical drive system output power, [kW]
$P_{\text{fuel}}$	fuel output power, [kW]
$P_{\text{prop}}$	propulsive output power, [kW]
$P_{\text{turb}}$	turbine engine output power, [kW]
$R_{\text{batt}}$	range of battery-based aircraft, [m]
$R_{\text{fuel}}$	range of fuel-based aircraft, [m]
$Se_{\text{batt}}$	battery specific energy, [Wh/kg] (in text) or [J/kg] (in equations)
$Se_{\text{fuel}}$	fuel specific energy, [Wh/kg] (in text) or [J/kg] (in equations)
$Sp_{\text{elec}}$	electric drive specific power, [kW/kg]
$v_{\text{cruise}}$	cruise velocity, [m/s]
$W_{\text{batt}}$	battery weight, [N]
$W_i$	cruise weight of aircraft, initial value, [N]
$W_f$	cruise weight of aircraft, final value, [N]
$W_{\text{elec}}$	electric drive weight, [N]
$W_{\text{fuel}}$	aircraft fuel weight, [N]
$W_{\text{payload}}$	payload weight, [N]
$W_{\text{OEW}}$	operating empty weight of aircraft, [N]
$\alpha$	ratio of takeoff to cruise power
$\eta_{\text{elec}}$	efficiency of electric drive system
$\eta_o$	overall aircraft efficiency
$\eta_{\text{prop}}$	propulsive efficiency of aircraft
$\eta_{\text{therm}}$	thermal efficiency of turbine engine
$\zeta$	electric propulsion fraction

## References

- [1] R. H. Jansen et al., "Turboelectric aircraft drive key performance parameters and functional requirements," presented at the 51st AIAA/SAE/ASEE Joint Propulsion Conf., Reston, VA, 2015, Paper AIAA 2015-3890.
- [2] R. H. Jansen, K. P. Duffy, and G. V. Brown, "Partially turboelectric aircraft drive key performance parameters," presented at the 53rd AIAA/SAE/ASEE Joint Propulsion Conf., Atlanta, GA, 2017, Paper AIAA 2017-4702.
- [3] J. L. Felder et al., "Turboelectric distributed propulsion engine cycle analysis for hybrid-wind-body aircraft," presented at the 47th AIAA Aerosp. Sci. Mtg., Orlando, FL, 2009, Paper AIAA 2009-1132.
- [4] G. V. Brown, "Weights and efficiencies of electric components of a turboelectric aircraft propulsion system," presented at the 49th AIAA Aerosp. Sci. Mtg., Orlando, FL, 2011, Paper AIAA 2011-225.
- [5] J. L. Felder et al., "Turboelectric distributed propulsion in a hybrid wind body aircraft," presented at the 20th Intl. Soc. for Airbreathing Engines Meeting, Gothenburg, Sweden, 2011, Paper ISABE-2011-1340.

- [6] A. T. Wick et al., "Integrated aerodynamic benefits of distributed propulsion," presented at the 53rd AIAA Aerosp. Sci. Mtg., Kissimmee, FL, 2015, Paper AIAA 2015-1500.
- [7] R. H. Jansen, C. Bowman, and A. Jankovsky, "Sizing power components of an electrically driven tail cone thruster range extender," presented at the 16th AIAA Aviation, Tech., Integration, and Ops. Conf., Washington, DC, 2016, Paper AIAA 2016-3766.
- [8] T. P. Dever et al., "Assessment of technologies for noncryogenic hybrid electric propulsion," NASA, Cleveland, OH, Tech. Rep. GRC-E-DAA-TN10454, 2015.
- [9] J. Welstead and J. L. Felder, "Conceptual design of a single-aisle turboelectric commercial transport with fuselage boundary layer ingestion," presented at the 54th AIAA Aerospace Sci. Meeting, San Diego, CA, 2016, Paper AIAA 2016-1027.
- [10] K. R. Antcliff and F. M. Capristan, "Conceptual design of the parallel electric-gas architecture with synergistic utilization scheme (PEGASUS) concept," presented at the 18th AIAA/ISSMO Multidisciplinary Analysis and Optimization Conf., Denver, CO, 2017, Paper AIAA 2017-4001.
- [11] K. R. Antcliff et al., "Mission analysis and aircraft sizing of a hybrid-electric regional aircraft," presented at the 54th AIAA Aerosp. Sci. Mtg., San Diego, CA, 2016, Paper AIAA 2016-1028.
- [12] M. Hepperle, "Electric flight – potential and limitations," presented at the Energy Efficient Tech. and Concepts of Operation Workshop, Lisbon, Portugal, 2012, Paper STO-MP-AVT-209.